

Synthesis and characterization of Fe₃O₄-HfO₂ nanoparticles by hyperfine interactions measurements

Cite as: AIP Advances **11**, 015047 (2021); <https://doi.org/10.1063/9.0000235>

Submitted: 16 October 2020 . Accepted: 12 December 2020 . Published Online: 28 January 2021

 T. S. N. Sales,  A. Burimova, P. S. Rodrigues, I. T. Matos,  G. A. Cabrera-Pasca,  R. N. Saxena, L. F. D. Pereira, L. Otubo, and  A. W. Carbonari

COLLECTIONS

Paper published as part of the special topic on [65th Annual Conference on Magnetism and Magnetic Materials](#), [65th Annual Conference on Magnetism and Magnetic Materials](#), [65th Annual Conference on Magnetism and Magnetic Materials](#), [65th Annual Conference on Magnetism and Magnetic Materials](#), [65th Annual Conference on Magnetism and Magnetic Materials](#) and [65th Annual Conference on Magnetism and Magnetic Materials](#)



View Online



Export Citation



CrossMark

ARTICLES YOU MAY BE INTERESTED IN

[Local inspection of magnetic properties in GdMnIn by measuring hyperfine interactions](#)

AIP Advances **11**, 015322 (2021); <https://doi.org/10.1063/9.0000037>

[Highly-sensitive magnetic sensor for detecting magnetic nanoparticles based on magnetic tunnel junctions at a low static field](#)

AIP Advances **11**, 015046 (2021); <https://doi.org/10.1063/9.0000189>

[Time dependence of magnetic moment of strontium-ferrite powder measured with a biaxial vibrating sample magnetometer \(VSM\)](#)

AIP Advances **11**, 015048 (2021); <https://doi.org/10.1063/9.0000216>

AIP Advances

Photonics and Optics Collection

READ NOW!



Synthesis and characterization of $\text{Fe}_3\text{O}_4\text{-HfO}_2$ nanoparticles by hyperfine interactions measurements

Cite as: AIP Advances 11, 015047 (2021); doi: 10.1063/9.0000235
Presented: 6 November 2020 • Submitted: 16 October 2020 •
Accepted: 12 December 2020 • Published Online: 28 January 2021



T. S. N. Sales,^{1,a)} A. Burimova,¹ P. S. Rodrigues,¹ I. T. Matos,¹ G. A. Cabrera-Pasca,² R. N. Saxena,¹ L. F. D. Pereira,¹ L. Otubo,¹ and A. W. Carbonari¹

AFFILIATIONS

¹Instituto de Pesquisas Energéticas e Nucleares, IPEN-CNEN/SP, São Paulo, SP 05508-000, Brazil

²Universidade Federal do Pará, Abaetetuba, PA 68440-000, Brazil

Note: This paper was presented at the 65th Annual Conference on Magnetism and Magnetic Materials.

a) Author to whom correspondence should be addressed: tatianenas1@gmail.com

ABSTRACT

Nanoparticles (NPs) that combine biocompatibility and enhanced physical characteristics for biomedical applications are currently an area of intense scientific research. Hafnium oxide NPs are an innovative approach in the anticancer treatment by radiotherapy due to their low toxicity and enhancement of local dose in the tumor reducing the total radiation dose for the patient. The combination of this property with the excellent magnetic hyperthermia performance of Fe_3O_4 NPs can produce a promising nanomaterial for cancer therapy. In this work, we attempted to synthesize nanoscale samples of HfO_2 doped with nominal 10 at.% Fe, and Fe_3O_4 doped with Hf at 10 at.% level using simple chemical routes. The crystal structure of the samples was characterized by X-ray diffraction. The material was irradiated with neutrons in a research reactor, the nuclear reaction $^{180}\text{Hf}(n, \gamma)^{181}\text{Hf}$ yielding the probe nucleus $^{181}\text{Hf}(^{181}\text{Ta})$ used in the perturbed angular correlations experiments to measure hyperfine interactions. Despite their immediate response to the external magnetic field, at local level both samples showed only electric quadrupole interaction typical of the monoclinic hafnia indicating that Fe replaces Hf in HfO_2 NPs, but, rather than substituting Fe, Hf enters magnetite in the form of HfO_2 clusters. Transmission Electron Microscopy was exploited to study the morphology of these complex systems, as well as to localize hafnia clusters and understand the nature of their coupling to Fe_3O_4 specks.

© 2021 Author(s). All article content, except where otherwise noted, is licensed under a Creative Commons Attribution (CC BY) license (<http://creativecommons.org/licenses/by/4.0/>). <https://doi.org/10.1063/9.0000235>

I. INTRODUCTION

Magnetite nanoparticles (NPs) are known for their extended applications, among which is their employment in biomedicine.¹ In this connection they are mostly known as imaging, delivery and hyperthermia agents.^{2,3} The latter two are, obviously, complementary.

In turn, nanoscale hafnia was recently recognized as an excellent candidate for radiotherapy.⁴ With its high atomic number $Z = 72$, Hf delivers an enhanced radiation dose to target cells, whereas the nontoxicity of HfO_2 minimizes the damage to healthy tissue. After the successful tests, the effect in patients is being clinically evaluated demonstrating good performance and safety profile.⁵

Therefore, composite $\text{Hf}_x\text{Fe}_y\text{O}$ (HFO) NPs, with radioenhancers and preserved magnetic properties of Fe_3O_4 , are expected

to suit for a simultaneous hyperthermia and radiotherapy treatment, as well as to allow an easy magnetically controlled delivery.

Apparently, the optimal HFO NP design is that with magnetite core (to preserve magnetic properties) and hafnia shell (taking the advantage of both its biocompatibility and radiosensitivity) of moderate thickness. Substitutional doping with Hf at Fe site of Fe_3O_4 in reasonable proportion may also be an option for such functionalization. However, one has to bear in mind structural differences of HfO_2 and Fe_3O_4 phases, and that Hf@Fe is at the edge of Hume-Rothery atomic radii and valence criteria. The least attractive HFO design is likely Fe@Hf in HfO_2 , although the study of $\text{Fe}_x\text{Hf}_{1-x}\text{O}_2$ is of interest both as complementary to $\text{Hf}_x\text{Fe}_{3-x}\text{O}_4$, and as a contribution to long-standing debate over the magnetism in hafnia.⁶

To understand the limitations in the design of composite nanoscale material on Fe-Hf basis for combining hyperthermia with radiotherapy, and the challenges associated with the control over its quality, we adopted simple routes to synthesize Fe-doped HfO_2 and Hf-doped Fe_3O_4 NPs. The properties of the materials were probed with conventional characterization methods, as well as hyperfine interactions based nuclear technique, perturbed angular correlation (PAC) spectroscopy, known for its successful application to the investigation of magnetism in nanomaterials.⁷

II. METHODOLOGY

A. Synthesis

Fe-doped HfO_2 sample, further referred to as $\text{Hf}^{(\text{Fe})}$, with nominal iron concentration of 10 at.%, was synthesized via the classic sol-gel route with metallic Hf and Fe as precursors dissolved in HF and HNO_3 stock solutions respectively. The method implied calcination at 823 K in air.

Nominal $\text{Hf}_{0.1}\text{Fe}_{2.9}\text{O}_4$, denominated $\text{Fe}^{(\text{Hf})}$, was synthesized via coprecipitation. Metallic hafnium dissolved in HF was first mixed with FeCl_2 in purified deionized deaerated (P-DI-D) H_2O under mechanical stirring. Then FeCl_3 was added, in adequate proportion to form $\text{Hf}_{0.1}\text{Fe}_{1.1}^{2+}\text{Fe}_{1.8}^{3+}\text{O}_4$. The addition of ammonia water resulted in immediate formation of black precipitate. After 40 minute stirring, it was separated magnetically from the solution and washed several times in P-DI-D water, analytical grade acetone, and then dried in vacuum.

Unlike $\text{Hf}^{(\text{Fe})}$, $\text{Fe}^{(\text{Hf})}$ has shown immediate response to the external magnetic field.

The sample of the second bunch was separated in two parts, one remaining intact and the other subjected to annealing. A typical procedure implied 12 hour treatment in vacuum at 773–823 K followed by natural cooling. The magnetic responses of the samples remained unchanged after annealing.

B. Characterization

X-ray diffraction patterns were collected partially at Bruker D8 Advance 3kW diffractometer and partially at Rigaku Mini-Flex II with $\text{Cu K}\alpha$ radiation, $\lambda = 1.5418\text{\AA}$. Rietveld refinement was performed using GSAS II software.^{8,9}

Transmission electron microscopy images were taken at JEM-2100 by Jeol and processed with ImageJ complemented by MATLAB scripts developed by the authors.

The less common PAC spectroscopy is based on the correlation between the directions of two subsequent gamma emissions from a radioactive probe. Relative direction and time between the emissions are coupled to the perturbation of probe nuclei states by the surrounding hyperfine fields. Thus, measurements of the evolution of the spin-rotation function $R(t) = A_{22}G_{22}(t)$, with $G_{22}(t)$ being the perturbation function, allow extracting information on local electromagnetic fields around the probe.¹⁰

In this study, a conventional $90^\circ/180^\circ$ geometry consisting of 4 BaF_2 detectors combined with a slow-fast coincidence timing electronics was used. The native element of the samples, i. e., Hf, was exploited to produce the ^{181}Hf parent of ^{181}Ta PAC probe. In order to activate Hf, vacuum sealed $\text{Hf}^{(\text{Fe})}$ and $\text{Fe}^{(\text{Hf})}$ samples

were exposed to $\sim 3.5 \times 10^{12} \text{ n cm}^{-1} \text{ s}^{-1}$ neutron flux in the IEA-R1 research reactor of IPEN for 8 hours.

III. RESULTS AND DISCUSSION

The experimental and refined X-ray diffraction (XRD) data obtained for $\text{Hf}^{(\text{Fe})}$ sample is shown in Fig. 1. It has revealed monoclinic HfO_2 (*m*- HfO_2) phase with space group $P12_1/c1$ (PDF 43-1017). According to XRD, the substitution of Hf ions by Fe has occurred in the sample causing a subtle positive chemical pressure. Also, Fe catalyzed the crystallite growth driven by elevated temperature at calcination, which was established via comparison with bare HfO_2 .

Concerning as synthesized $\text{Fe}^{(\text{Hf})}$, its diffraction pattern allowed to distinguish $Fd3m$ magnetite structure (PDF 19-629) and estimate the average crystallite size to be near 11 nm. (11-1) and (111) reflections testify the crystallization of hafnia into clusters of monoclinic phase upon annealing of this sample. The formation of $\alpha\text{-Fe}_2\text{O}_3$ (PDF 33-664) in a small proportion becomes evident due to the (104) reflection. The estimated size of HfO_2 clusters is 11 nm, whereas that of magnetite and hematite particles reach $\sim 38 \text{ nm}$. Although the main part of Hf was found to be aggregated in clusters, lattice constant of the main magnetite phase increases from 8.382 to 8.412 \AA upon annealing, which possibly indicates to the incorporation of a small amount of Hf ions into the structure.

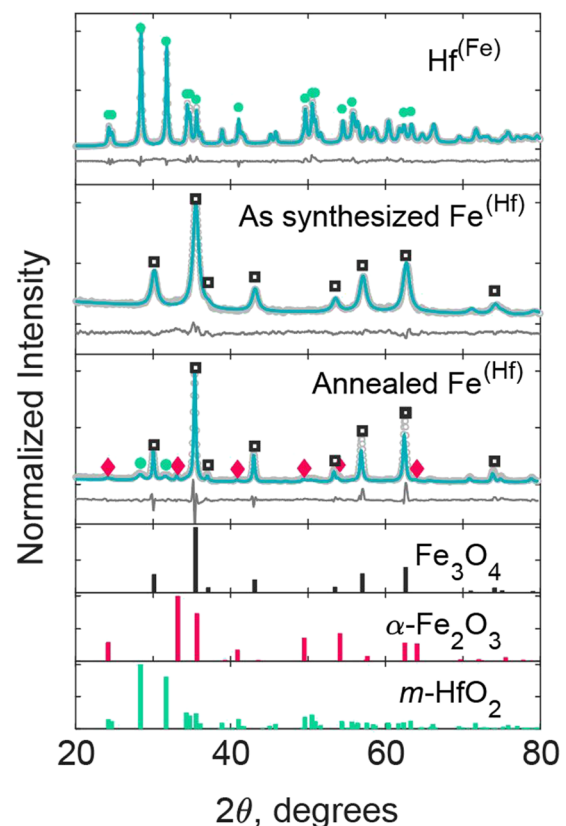


FIG. 1. XRD experimental and refined data obtained for the $\text{Hf}^{(\text{Fe})}$ sample and for $\text{Fe}^{(\text{Hf})}$ after synthesis and after annealing.

Moreover, the atomic order in hafnia is known to be distorted by defects, principally oxygen vacancies, when the speck size is smaller than 4 nm, so that the grains appear to be XRD-amorphous at this scale. We therefore assume the formation of smaller amorphous hafnia clusters at synthesis which is represented by the “background” halo of as synthesized $\text{Fe}^{(\text{Hf})}$ XRD pattern.

It should be pointed out that although XRD allows to understand the overall nature of doping, i.e., to evidence the preference of oxide cluster formation over ion substitution, it does not help localizing hafnia agglomerates. Their localization, however, is crucial to evaluate the potential of the material for a combined hyperthermia-radiotherapy treatment.

Local structure of the samples and its evolution upon annealing was probed with Time Differential (TD) PAC, are shown in Fig. 2.

Although the leading fraction in both $\text{Hf}^{(\text{Fe})}$ and $\text{Fe}^{(\text{Hf})}$ samples was that of $m\text{-HfO}_2$ ($\nu_Q = 789$ MHz, $\eta = 0.34$) with slightest variation in values from one sample to another, its contribution changed from 66.7% in $\text{Hf}^{(\text{Fe})}$ to 51% in annealed $\text{Fe}^{(\text{Hf})}$. Note that the complementary frequency (41%) observed for $\text{Fe}^{(\text{Hf})}$ is distributed very broadly ($\delta = 33\%$). Attributing it to the distorted site at the NP surface and taking into account the fact that HfO_2 NPs stabilize in monoclinic structure at their characteristic sizes ≥ 5 nm (below that metastable structures like orthorhombic and tetragonal, $t\text{-HfO}_2$, are preferential), assuming the clusters to be spherical for simplicity, one estimates the speck size of $\text{Fe}^{(\text{Hf})}$ as moderately above 6.3 nm, which is in good agreement with XRD results.

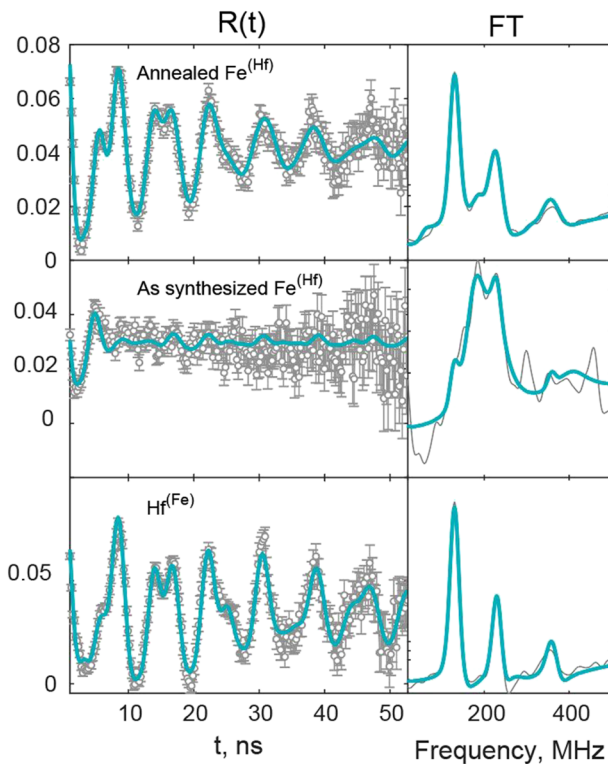


FIG. 2. PAC spectra of $\text{Fe}^{(\text{Hf})}$ (top) and $\text{Hf}^{(\text{Fe})}$ (bottom) together with their Fourier Transforms (right).

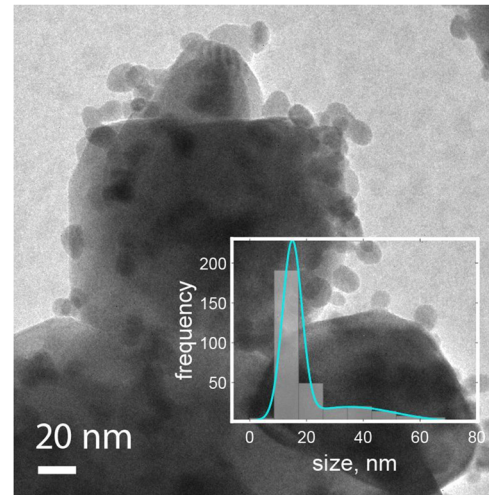


FIG. 3. TEM image of the $\text{Fe}^{(\text{Hf})}$ sample after annealing and corresponding size distribution histogram. Note that other images were also considered to plot particle size distribution.

Most notable of TDPAC results, however, is that neither of the samples showed magnetic hyperfine contribution expected in Fe_3O_4 . This implies the situation of Hf ions almost entirely at HfO_2 or at the sites with low degree of ionic spin ordering, like domain walls and surfaces.

The problem of localization of HfO_2 clusters in $\text{Fe}^{(\text{Hf})}$ was further approached with TEM. First, as shown in Fig. 3, the annealing of $\text{Fe}^{(\text{Hf})}$ was detected to result in the formation of core-satellite objects with the characteristic core size estimated to be 40 nm on average

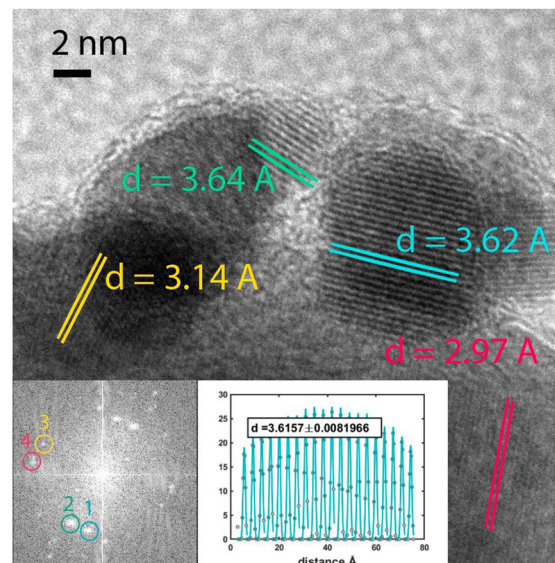


FIG. 4. TEM image of the $\text{Fe}^{(\text{Hf})}$ sample showing the interplanar distances. The insets demonstrate FFT and multiple-Gaussian approximation used in the calculation of d -spacing.

and ~15 nm satellites, coinciding with XRD estimation for Fe_3O_4 and HfO_2 in the annealed hafnium doped magnetite sample.

A meticulous analysis of d -spacing in a series of TEM images was performed in order to establish the structural composition of the cores and the satellites. In accordance with XRD, TEM analysis gives lower values of interplanar distances for the sample before annealing, compared to the annealed material, though the difference is more expressive than that predicted by the diffraction measurements. On the basis of 22 picked sets of lattice planes at different TEM images, we hypothesized that the cores consist of Fe_3O_4 domains, whereas the satellite particles in their majority have the structures close to m - and t - HfO_2 and, to a less extent, hematite. An example of the results is shown in Fig. 4. We are aware, however, of the restricted representativeness of this assumption due to the small sampling volume.

IV. CONCLUSIONS

Although the core-shell structure might be ideal for hyperthermia-radiotherapy targeted HFO NPs, likely, any form of nano magnetite-attached hafnia clusters may suit for such complex therapy. It is not trivial, however, to establish whether HfO_2 and Fe_3O_4 specks are anyhow fixed to each other when no substitutional doping occur. In this work we have shown the challenges at the preparation of HFO systems, as well as the possibilities and limitations of conventional and exclusive techniques in detecting the attachment of hafnia clusters to magnetite.

Since smaller HfO_2 clusters are amorphous, conventional methods fail localizing them in the as synthesized NPs. The locality of PAC spectroscopy is restricted to spotting the distorted phase along with crystalline m - HfO_2 . High resolution TEM suggested satellite hafnia, but did not close the discussion because of the small sampling and non-statistical measurement errors.

Importantly, we emphasize that the core-satellite arrangement may be preliminary to the desired core-shell structure. Further research is to be conducted to adjust the synthesis parameters, among which annealing time and temperature, for attaining optimal satellite density, fewer-domain cores and adequate core-satellite size ratio.

ACKNOWLEDGMENTS

Partial financial support for this work was provided by Fundação de Amparo a Pesquisa do Estado de São Paulo (FAPESP) under grant 2017/50332-0. A.W.C. and R.N.S. acknowledge the Conselho Nacional de Desenvolvimento Científico e Tecnológico (CNPq) for financial support in a form of research fellowship (grant 304627/2017-8). A.B. greatly acknowledges the financial support of

FAPESP (grant 2019/15620-0). T.S.N.S. acknowledges financial support from Comissão Nacional da Energia Nuclear (CNEN). P.S.R. acknowledges financial support from CNPq (grant 134423/2019-4). The authors would also like to express their great appreciation of the support from CNEN under grant 01342.002349/2019-96.

The authors thank Dr. R. H. L. Garcia for performing some of the XRD experiments, and Professor Dr. M. C. Felinto for providing access to the equipment and a continuous assistance in complementary XRD studies. The authors also express their gratitude to Professor Dr. F. A. Genezini and P. S. C. Silva for valuable discussions.

DATA AVAILABILITY

The data that support the findings of this study are available from the corresponding author upon reasonable request.

REFERENCES

- Y. Shen, J. Lifante, E. Ximendes, H. D. A. Santos, D. Ruiz, B. H. Juárez, I. Zabala Gutiérrez, V. Torres Vera, J. Rubio Retama, E. Martín Rodríguez, D. H. Ortigies, D. Jaque, A. Benayas, and B. del Rosal, "Perspectives for Ag_2S NIR-II nanoparticles in biomedicine: From imaging to multifunctionality," *Nanoscale* **11**, 19251–19264 (2019).
- L. Shen, B. Li, and Y. Qiao, " Fe_3O_4 nanoparticles in targeted drug/gene delivery systems," *Materials* **11**, 324 (2018).
- Y. V. Kolen'ko, M. Bañobre-López, C. Rodríguez-Abreu, E. Carbó-Argibay, A. Sailsman, Y. Piñeiro-Redondo, M. F. Cerqueira, D. Y. Petrovykh, K. Kovnir, O. I. Lebedev, and J. Rivas, "Large-scale synthesis of colloidal Fe_3O_4 nanoparticles exhibiting high heating efficiency in magnetic hyperthermia," *The Journal of Physical Chemistry C* **118**, 8691–8701 (2014).
- L. Maggiorella, G. Barouch, C. Devaux, A. Pottier, E. Deutsch, J. Bourhis, E. Borghi, and L. Levy, "Nanoscale radiotherapy with hafnium oxide nanoparticles," *Future Oncology* **8**, 1167–1181 (2012).
- C. L. Tourneau *et al.*, "NBTXR3 for the treatment of elderly frail patients with locally advanced HNSCC," *International Journal of Radiation Oncology Biology Physics* **105**, S54–S55 (2019).
- J. M. D. Coey, M. Venkatesan, P. Stamenov, C. B. Fitzgerald, and L. S. Dorneles, "Magnetism in hafnium dioxide," *Phys. Rev. B* **72**, 024450 (2005).
- I. T. Matos, B. Bosch-Santos, G. A. Cabrera-Pasca, and A. W. Carbonari, "Magnetic behavior of La-doped Fe_3O_4 studied by perturbed angular correlation spectroscopy with ^{111}Cd and ^{140}Ce ," *Journal of Applied Physics* **117**, 17D511 (2015).
- GSAS-II: The genesis of a modern open-source all purpose crystallography software package," in *Electronic Archive New Semiconductor Materials. Characteristics and Properties* (St. Petersburg, 2001).
- B. H. Toby and R. B. V. Dreele, "GSAS-II: The genesis of a modern open-source all purpose crystallography software package," *Applied Crystallography* **46**, 545–559 (2013).
- A. W. Carbonari, J. Mestnik-Filho, R. N. Saxena, and M. V. Lalić, "Magnetic hyperfine interaction in CeMn_2Ge_2 and CeMn_2Si_2 measured by perturbed angular correlation spectroscopy," *Phys. Rev. B* **69**, 144425 (2004).